Available online at www.sciencedirect.com
SCIENCE DIRECT
Trans. Nonferrous Met. Soc. China 16(2006) 98−104
Transactions of Nonferrous Metals Society of China
www.csu.edu.cn/ysxb/

Aging microstructural characteristics of ZA-27 alloy and SiC_p/ZA-27 composite

LI Zi-quan(李子全), ZHOU Heng-zhi(周衡志), LUO Xin-yi(骆心怡), WANG Tao(汪 涛), SHEN Kai(沈 凯)

College of Materials Science and Technology, Nanjing University of Aeronautics and Astronautics, Nanjing 210016, China

Received 15 August 2005; accepted 18 November 2005

Abstract: The aging characteristics of as-quenched microstructures of ZA-27 alloy and SiC_p/ZA-27 composite(ZMC_p) were investigated using SEM, EDS and TEM. The structure, morphology and size of sub-grains in primary dendrite in ZMC_p continuously change during aging process. Little tiny spherical Zn-rich η phase distributes in the dendrite. Amount of transitional α' phase, well coherent with equilibrium α_f phase, in SiC_p-neighboring dendrite edge zone is less than that in dendrite center zone. Both eutectic and peritectic β phase transform into lamellar α and η phases, obeying $[\bar{2}113]_\eta /\!/ [110]_\alpha$, and $(002)_\alpha /\!/ (1\bar{1}01)_\eta$. In the like-eutecticum of ZMC_p, less amount of β phase and decomposition products are found. The size of α phase decomposed from peritectic β phase in ZMC_p is obviously larger than that in the monolithic alloy. The lamella decomposition of β phase beside SiC_p is evidently more rapid than that in the alloy. SiC particulates strongly accelerate neighboring β phase decomposition in aging process.

Key words: SiC_p/ZA-27 composite; aging microstructure; ZA-27 alloy; precipitation; crystallographic orientation relationship

1 Introduction

Alloys, intermetallic compounds and metal matrix composites(MMC), processed by different solid solution and aging treatments, exhibit a variety of microstructures[1−5]. Influence of aging temperature and time on the phase structure, microstructures and mechanical properties of both alloys and MMCs have been widely studied[6−14].

Commercial Zn-Al foundry alloys and Zn alloy matrix composites have been of considerable industrial applications[15, 16]. However, one serious problem with these alloys and composites is a gradual and irreversible expansion that occurs over a period of time at ambient temperature, which worsens in harsh working conditions. This dimensional change is due to the conversion of metastable phases, which are retained by non-equilibrium solidification and solid-state transformation. Therefore, a solution-aging treatment was used in order to gain relative stable structure. Several investigations regarding the aging characteristics of hypo-eutectic and hyper-eutectic Zn-Al alloys have been performed using X-ray diffraction(XRD), optical microscopy(OM), differential scanning calorimetry (DSC) and scanning electronic microscopy(SEM)[17−23]. LI and CHAO[17] researched mechanical properties and aging characteristics of zircon-reinforced Zn-4Al-3Cu alloy at 95 ℃. They found that α phase precipitates from η phase at the initial stage of the aging process, and ε phase appears from η phase later on, furthermore the crystallographic orientation relation- ship between α and η phases is $[\bar{1}101]_\eta /\!/ [1\bar{1}0]_\alpha$ and $[11\bar{2}0]_\eta /\!/ (111)_\alpha$. SHARMA et al[21] investigated effect of aging parameters on the primary dendritic microstructure and properties of ZA-27/aluminite metal matrix composites. They indicated that the aging and precipitation kinetics in the matrix alloy are significantly accelerated due to the presence of particulate reinforcement, and therefore the changes in properties of the composites were explained on the basis of microstructure alterations during aging.

As mentioned above, almost all aging investigations of ZA-27 alloy were carried out without considering the inhomogeneity of the microstructure and composition. However, composition distributions in both as-cast ZA-27 alloy and its SiC particulate

Foundation item: Project(03G52047) supported by the Aviation Science Foundation, China
Corresponding author: LI Zi-quan; Tel: +86-25-84891343; E-mail: ziquanli@nuaa.edu.cn

reinforced composite are extremely inhomogeneous, due to the non-equilibrium solidification in fabrication process, which results in various microstructures in both materials[24]. So the variety of the microstructures and inhomogeneity of chemical compositions can not be ignored during the investigations on the aging process of both hypo-eutectic Zn-Al alloys and their composites.

In brief, the purpose of the present work is to investigate the effect of artificial aging conditions on the alterations of matrix microstructures and compositions for both ZA-27 alloy and SiC_p/ZA-27 composites(ZMC_p), as well as reveal the crystallographic orientation relationships between precipitation phases (or decomposition products) in both ZA-27 alloy and ZMC_p during aging processes using SEM, EDS and TEM.

2 Experimental

In present study, a Mg(1.0%, mass fraction) alloyed commercial foundry ZA-27 alloy was selected as the metal matrix of the composites, which had the chemical composition(mass fraction, %): Al 26−28, Cu 1.8−2.2, Mg 1.05−1.15, balance Zn. The ceramic particulate reinforcement was α-SiC particles with the size of 18 μm, received as abrasive grade. SiC_p/ZA-27 composite with SiC_p volume fraction of 10% was manufactured by application of mechanical electromagnetic combination stirring process(MECSP)[24]. The ZA-27 and ZMC_p samples were aged at 160 ℃ for 5, 15 and 20 h after solutionizing at 360 ℃ for 2 h by cold water chilling. The solutionized and quenched samples were kept at −20 ℃ before artificial aging.

The characteristics of microstructure and precipitation phases in both materials after aging treatment were observed using SEM (HITACHI X-650) at the accelerating voltage of 20 kV, EDS (attached to the SEM) and TEM (JEM-2000EX) at the accelerating voltage of 160 kV.

The dimension of SEM specimens for micrography was d10 mm×10 mm. Their surfaces were ground on SiC papers till to 600 grit. Then fine polishing was done using magnesium oxide paste followed by diamond paste on a velvet cloth. Etchant used was alcoholic solutions of nitric acid with volume fraction of 4%. The TEM specimens with 0.2 mm in thickness were firstly mechanically ground and polished to about 20 μm in thickness, then punched into d3 mm thin flakes, and finally reduced on a double-jet ion-milling (Gatan 600-TMP).

3 Results and discussion

The typical microstructures of ZA-27 and ZMC_p aged for different durations are shown in Fig.1 and Fig.2, respectively. The both matrix microstructures in cold-water chilling can be divided into three typical types, namely Al-supersaturated phase α'_s (dark, original primary dendrites), like-eutecticum $\alpha+\beta$ (white zones), and β phase (white strip around the original primary dendrite α) in Fig.1(a) and Fig.2(a), respectively. α phase is aluminum-rich phase, η phase is zinc-rich phase, and β phase, ZnAl, is intermetallic compounds. EDS results of the phases or microstructures in ZA-27 and ZMC_p aged for 5 h are listed in Tables 1 and 2, respectively. The Zn contents range from 24% to 76% in the different microstructures for ZA-27, and from 29% to 82% for ZMC_p. The results indicate that the composition is extremely inhomogeneous either in ZA-27 or ZMC_p. A variety of microstructures and difference in the chemical composition are attributed to non-equilibrium casting conditions and can not be eliminated simply by solid solution process at higher temperatures.

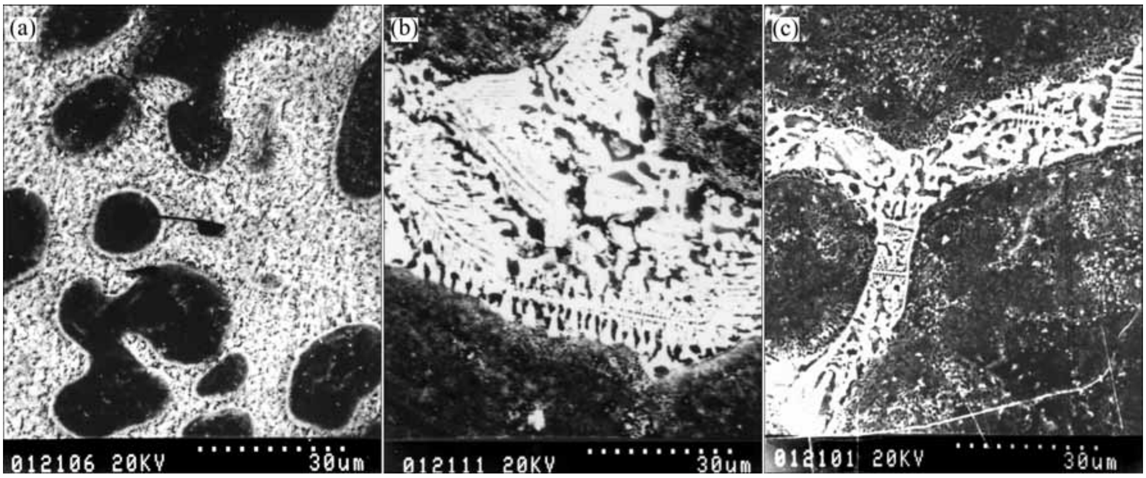

Fig.1 Microstructures of ZA-27 alloy aged for different durations: (a) 0 h; (b) 5 h; (c) 15 h

3.1 Decomposition microstructure of super-saturated α_s' phase

As stated above, high temperature over-saturated phase α_s' in both the monolithic alloy and ZMC_p, retained at ambient temperature due to rapid cooling, undergoes decomposition during artificial aging process. The Zn content gradually increases from 24% on the center of primary dendrite in ZA-27 to 29% on the edge, as listed in Table 1. Differently, the Zn content keeps about 29% along the dendrite in ZMC_p (Table 2). The Zn content indicates that in the primary dendrite of ZA-27 and ZMC_p only precipitation reaction can take place according to the Zn-Al phase diagram. Although there is no pronounced difference in micrograph at low magnification for the dendrite (Figs.1 and 2), changes of sub-grain morphology, size and crystal structure are confirmed by TEM in Fig.3, which shows typical microstructure images of the dendrite in the ZMC_p at as-quenched state and aged at 160 ℃ for 5 h. Near SiC particle, dendritic microstructure in as-quenched condition is composed of d100 nm×300 nm long column over-saturated phase α_s' (a=0.398 0 nm). The microstructure of the dendrite center zone in ZMC_p consists of white region and small amount of elliptical particles under same aging conditions (Fig.3(b)). The white region is characterized as stable Al-rich phase α_f (a=0.401 5 nm) by an electron diffraction pattern in 〈110〉 (Fig.4), which is decomposed from over-saturated phase α_s'. The elliptic particles are confirmed as α' (α= 0.399 2 nm, the transitional phase of α_f), which contains more Zn than equilibrium phase α_f. As no individual diffraction spots are found in Fig.4 and there is very small difference in their crystal lattice constants, α' keeps well coherent relationship with α_f. Lower aging temperature and shorter aging duration result in the incompleteness of the transition from α' to α_f. Some separated tiny secondary precipitates can also be found in Fig.5. They are confirmed as Zn-rich η

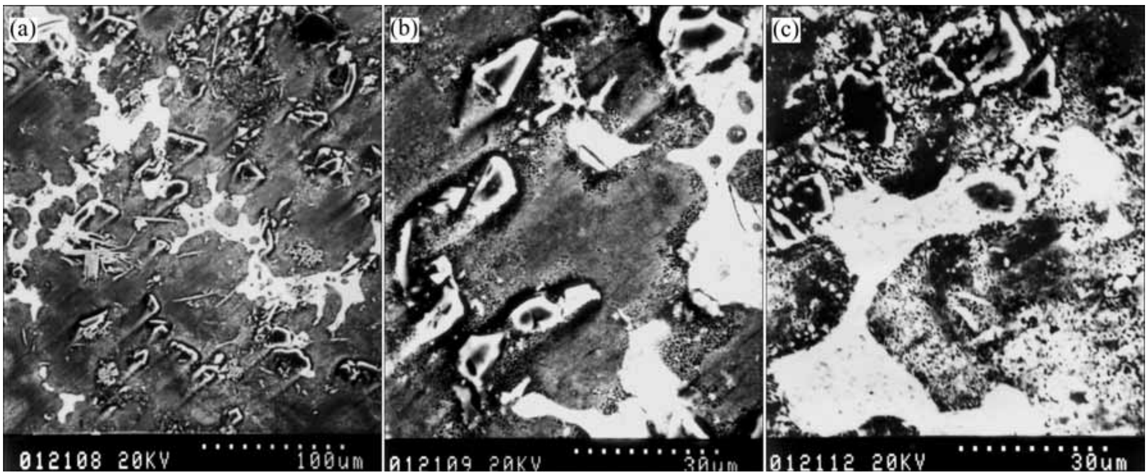

Fig.2 Microstructures of SiC_p/ZA-27 composites aged for different durations: (a) 0 h; (b) 5 h; (c) 20 h

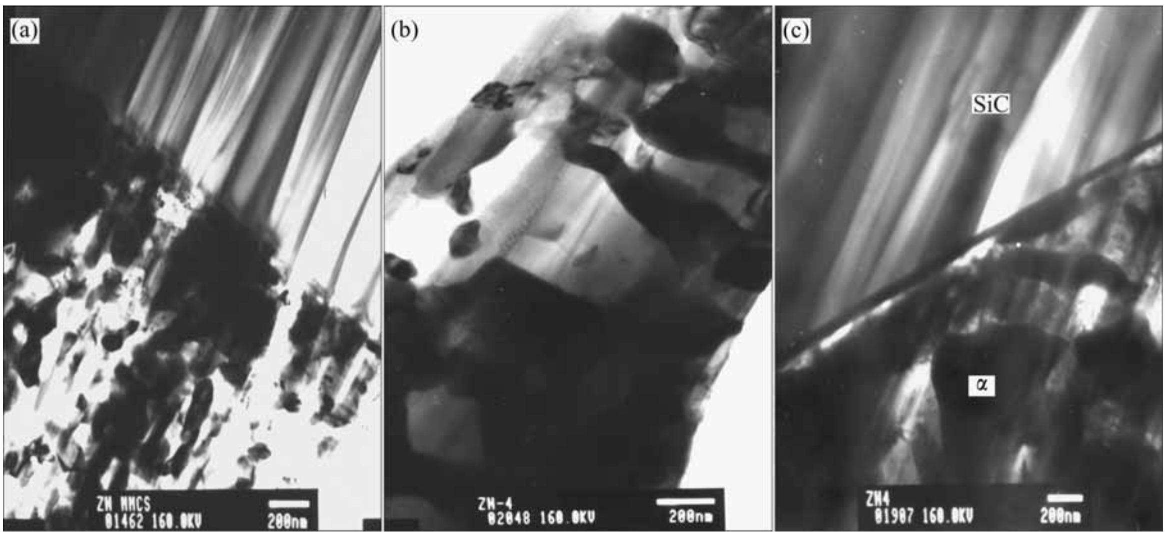

Fig.3 Typical microstructure images of dendrite in MMCs aged at 160 ℃: (a) As-quenched, 0 h; (b) At center, 5 h; (c) At edge, 5 h

Table 1 EDS elemental analysis of phases in ZA-27 alloy aged for 5 h (mass fraction, %)

Analysis method		Mg	Al	Cu	Zn
Spot analysis	White zone	0.20−0.22	12.0−15.50	13.40−14.70	70.91−76.42
	Dark zone	1.50−2.05	12.50−14.80	9.61−10.60	66.42−67.83
Area analysis		1.18	14.50	10.0	74.32
Verge of original dendrite/area analysis		0.78	66.02	3.76	29.44
Center of original dendrite/area analysis		0.77	73.75	1.76	23.72

Table 2 EDS elemental analysis of phases in MMCs aged for 5 h (mass fraction, %)

Analysis method		Mg	Al	Cu	Zn	Si
White zone	Spot analysis	5.68−2.78	3.04−3.12	9.84−9.97	81.11−81.92	
	Area analysis	5.48	3.54	9.84	81.14	
Verge of original dendrite near SiC/area analysis		0.78	62.91	2.89	29.13	4.29
Center of original dendrite/area analysis		0.51	68.98	1.69	28.82	

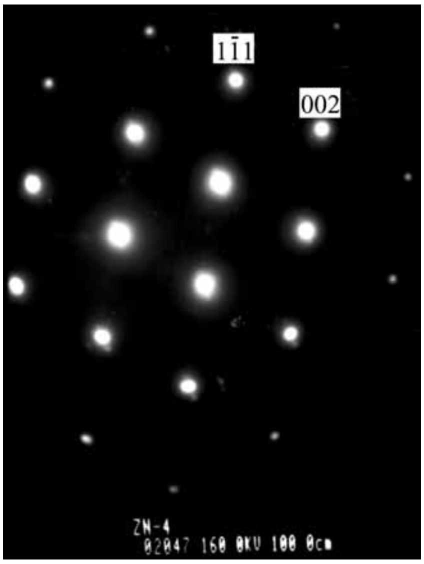

Fig.4 Electron diffraction pattern of α in 〈110〉

Fig. 5 Dark field image of MMCs matrix aged at 160 ℃ for 20 h

phase by accurate diffraction technology. The microstructure of dendrite edge zone neighboring SiC particle consists of equilibrium phase α_f, tiny η phase and very little amount of transitional phase α' (Fig.3(c)). The size of α_f in different regions is almost identical (about 500 nm). The results indicate that SiC particles in ZMC_p have little influence on grain growth, whereas facilitate precipitation in the local zone of over-saturated dendrite, which could be attributed to the Zn diffusion accelerating effect due to the tensile stress field in the matrix, because of the difference between matrix and SiC in coefficient of thermal expansion.

3.2 Changes of like-eutecticum

Microstructure of the like-eutecticum in ZA-27 alloy continuously changes with aging time (Fig.1). In as–quenched state, β phase (in dark) merely partially decomposes. Fig.6 shows TEM images of black and white lamellar structure of β (Zn 74.3%) decomposition products in the like-eutecticum of ZA-27 alloy aged for 5 h. During aging process, β phase in the like-eutecticum completely decomposes into (α+η) according to Fig.6, in which α and η phases are identified by electron diffraction patterns, and then the decomposition products form fishbone-like structure (η+(α+η)) with existing η phase, as shown in Fig.1. Multi-element lamellar microstructure (α+η), of which the synthesized electron diffraction patterns are shown in Fig.7, coarsened with the increase of aging time. In order to confirm the crystallographic orientation relationship between α and η, the electron diffraction patterns of α and η in [110] and [$\bar{2}$113], as well as their synthetic electron diffraction pattern are simulated with the standard crystallographic parameters of both α and η phases by a special simulation program, as shown in Fig.8. The simulated patterns fully agree with the experimental patterns in Fig.7, which indicates that the (002) crystal plane of α nearly parallels to (1$\bar{1}$01) crystal plane of η. Therefore, it can be surely confirmed that in the

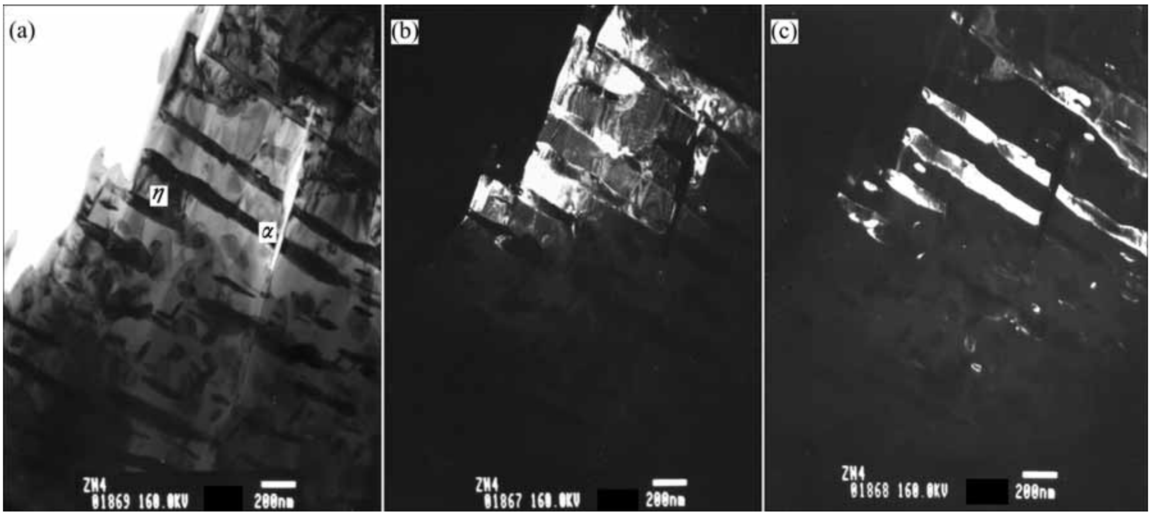

Fig.6 Images of lamellar structure of β phase decomposition in like-eutecticum of ZA-27 alloy aged for 5 h: (a) Bright field image; (b) Dark field image of η; (c) Dark field image of α

Fig.7 Synthetic electron diffraction pattern of α and η phases

lamellar structure the black noodle-like phase is α, while the continuous white one is η in the bright field image.

Comparing Fig.1 and Fig.2, amount of like-eutecticum in as-quenched composite is visibly less than that in as-quenched monolithic alloy. Less spherical decomposed β phase distributes in like-eutecticum. As shown in Fig.2, little decomposition product continuously precipitates and grows slowly with increase of aging time. It shows that like-eutecticum microstructure in ZMPs is relatively stable with regarding to ZA-27. One of reasons is that the aggregated Zn and lower Al content in the like-eutecticum (Tables 1 and 2) result from extremely high cooling rate and vigorous agitation during solidification process[24]. Therefore, the compositional deviation results in that less amount of β phase presented in the like-eutecticum in equili- brium conditions. Another reason is that much more amorphous oxides[24], formed in fabrication process, aggregated in the final solidification region. Consequently, efficient amount of alloy elements reduces, resulting in the reduction of β phase as well. Fig.9(a) shows image of lamellar structure of β phase decomposition products in the like-eutecticum of ZMCs aged for 5 h. The distribution of α and η phases are analogous to that in the monolithic alloy. But some spherical precipitates in the decomposed β phase can be observed in bright and dark field images, shown in Figs.9(a) and 9(b). Fig.9(c) shows an electron diffraction pattern of the precipitates in [111], by which the crystal structure of precipitation phase is determined as B_2 structure with lattice constant of a=0.294 nm. The precipitates are confirmed as CuZn, which was not found in as-cast materials[24].

3.3 Decomposition of peritectic β phase

Very small amount of peritectic β phase, around the primary dendrite in a thin-strip shape, is retained in both as-quenched materials (Fig.1(a) and Fig.2(a)). It transforms into lamellar two-phase structures in style of cellular decomposition (grey in Fig.1(b) and Fig.2(b)), and α phase gradually coarsens in the aging process. For the same aging time, the size of α phase in ZMC_p is obviously larger than that in the monolithic. Especially, lamellar decomposition reaction takes place more easily in β phase neighboring SiC particles and coarser α phase is gained in peritectic β phase of ZMC_p. This implies that the

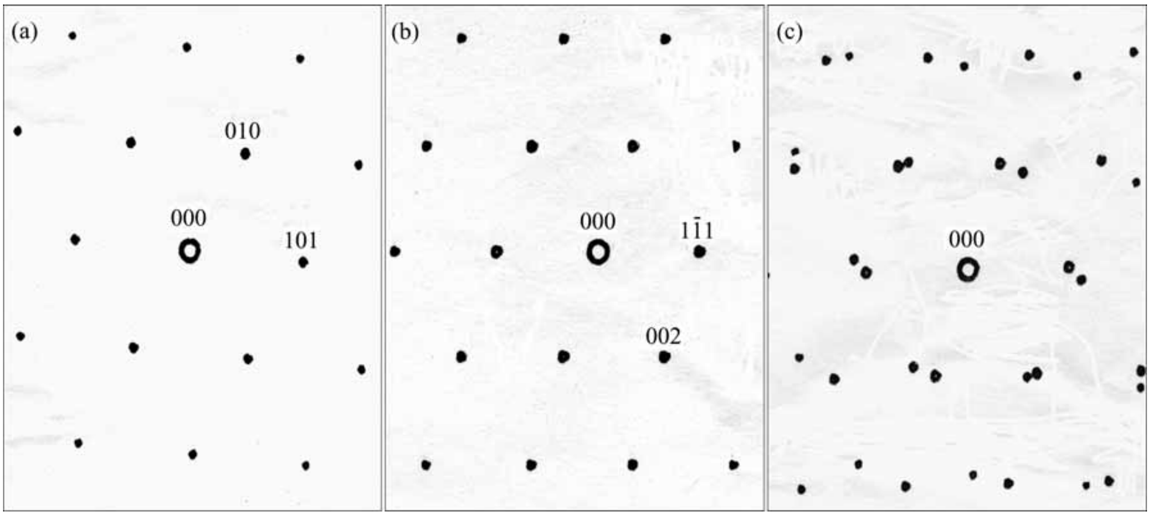

Fig. 8 Computer-simulated electron diffraction patterns of α and η as well as $\alpha+\eta$ in $[\bar{2}113]_\eta$ and $[110]_\alpha$: (a) $[\bar{2}113]_\eta$; (b) $[110]_\alpha$; (c) $[\bar{2}113]_\eta$ // $[110]_\alpha$

Fig. 9 TEM images of lamellar structure and electron diffraction pattern of CuZn in like-eutecticum of SiCp/ZA-27 composite aged for 5 h: (a) Bright field image; (b) Dark field image; (c) Electron diffraction pattern of CuZn in [111]

growth rate of α phase in ZMC_p is evidently higher than that in ZA-27 alloy, and SiC particles strongly hasten the decomposition of β phase.

4 Conclusions

1) Existence of SiC_p in matrix facilitates Zn and Cu diffusion and makes SiC-neighboured matrix transformation easier. Either eutectic or peritectic β phase transforms into lamellar α and η phases in style of cellular decomposition, obeying $[\bar{2}113]_\eta$ // $[110]_\alpha$, and $(002)_\alpha$ // $(1\bar{1}01)_\eta$.

2) Only precipitation reaction can occur in primary dendrite for both ZA-27 and ZMC_p. Al-supersatured α'_s continuously transforms into transitional phase α' and η(Zn), then α' transforms with well coherent relationship into stable α_f. Amount of α' in dendrite edge zone neighboring SiC_p is less than that in dendrite center zone.

3) Aggregated Zn and Cu as well as oxides in the like-eutecticum of ZMC_p result in less amount of β phase and form spherical precipitates CuZn. The like-eutecticum microstructure in ZMC_p is relatively stable.

4) The size of α phase decomposed from peritectic β phase in ZMC_p is obviously larger than that in the monolithic. The growth rate of α phase in ZMC_p is evidently higher than that in ZA-27, and SiC_p

strongly accelerate decomposition of peritectic β phase.

References

[1] MONAJATI H, JAHAZI M, BAHRAMI R, YUE S. The influence of heat treatment conditions on characteristics in Udimet[J]. Materials Science and Engineering A, 2004, 373: 286−293.

[2] JANG J S C, CHANG L J. Effect of heat treatment on the microstructure change and mechanical properties for the Ni-19Si-3Nb-0.15B intermetallic alloy[J]. Materials Chemistry and Physics, 2003, 82: 128−133.

[3] YI Fen-ga, NING Tao, ZHU Zhen-gang, HU Shi-sheng, PAN Yi. Effect of aging treatment on the quasi-static and dynamic compressive properties of aluminum alloy foams[J]. Materials Letters, 2003, 57: 4058−4063.

[4] WU Gao-hui, YU Zhi-qiang, SUN Dong-li, ZHANG Hui. Rare-earth modification of sub-micron Al_2O_3 particle surface and its effect on the aging behavior of 6061Al composite[J]. Acta Metallurgica Sinica, 2003, 39(8): 870−874.

[5] ZHENG M Y, WU K, KAMADO S, KOJIMA Y. Aging behavior of squeeze cast SiC/AZ91 magnesium matrix composite[J]. Materials Science and Engineering A, 2003, 348: 67−75.

[6] ZHOU Y C, LONG S G, LIU Y W. Thermal failure mechanism and failure threshold of SiC particle reinforced metal matrix composites induced by laser beam[J]. Mechanics of Materials, 2003, 35: 1003−1020.

[7] KIOURTSIDIS G E, SKOLIANOS S M, LITSARDAKIS G A. Aging response of aluminium alloy 2024/silicon carbide particles (SiC_p) composites[J]. Materials Science and Engineering A, 2004, 382: 351−361.

[8] ZHANG F, SUN P F, LI X C. An experimental study on deformation behavior below 0.2% offset yield stress in some SiC_p/Al composites and their unreinforced matrix alloys[J]. Materials Science and Engineering A, 2001, 300: 12−21.

[9] LI Y Y, ZHANG W W, FEI J, ZHANG D T, CHEN W P. Heat treatment of 2024/3003 gradient composite and diffusion behavior of the alloying elements[J]. Materials Science and Engineering A, 2005, 391: 124−130.

[10] DAOUD A, REIF W. Influence of Al_2O_3 particulate on the aging response of A356 Al-based composites[J]. Journal of Materials Processing Technology, 2002, 123: 313−318.

[11] BI Y, WANG R C, LI W X, LIU Z S. Study on thermomechanical treatment of SiC_p/6066Al composites[J]. Aluminium Machining, 2004, 156: 7−11, 14.

[12] JIANG L T, ZHAO M, WU G H, ZHANG Q. Aging behavior of sub-micron Al_2O_{3p}/2024Al composites[J]. Materials Science and Engineering A, 2004, 392: 366−372.

[13] BEKHEETA N E, GADELRABB R M, SALAHC M F, ABDEI-AZIM A N. The effects of aging on the hardness and fatigue behavior of 2024 Al alloy/SiC composites[J]. Materials and Design, 2002, 23: 153−159.

[14] XIE S H, LIU H W, CHEN K H, LI J Q, TANG J N. The influence of solution hardening and aging treatment on thermal conductivity and strength of SiC_p/6013Al composite with high SiC_p particles content[J]. Hunan Metallurgy, 2003, 31(3): 16−19.

[15] LI Z Q, WU B Y, ZHANG S Y. Pretreatment process of SiC particles and fabrication technology of SiC particulate reinforced Zn-Al alloy matrix composite[J]. Materials Science and Technology, 2001, 17(8): 954−960.

[16] PRASAD B K. Abrasive wear characteristics of a zinc-based alloy and zinc-alloy/SiC composite[J]. Wear, 2002, 252: 250−263.

[17] LI B J, CHAO C G. Mechanical properties and 95 ℃ aging characteristics of zircon-reinforced Zn-4Al-3Cu alloy[J]. Metallurgy and Materials Transaction, 1996, 27(3): 809−818.

[18] SAVASKAN T. Decomposition of Zn-Al alloys on quench-aging[J]. Materials Science and Technology, 1990(8): 695−703.

[19] WEI S Z. Study of aging process of ZnAl27Cu2Mg0.01 alloy[J]. Transaction of Luoyang Engineering College, 1993(3): 58−62.

[20] ZHU Y H. Decomposition reactions in a chilling-aged eutectoid (Zn-Al Based Alloy AlZn75Cu3Si2)[J]. Journal of Materials Science, 1990, 32(1): 125−131.

[21] SHARMA S C, SHANTA S, KRISHNA M. Effect of aging parameter on the microstructure and properties of ZA-27/aluminite metal matrix composites[J]. Journal of Alloys and Compounds, 2002, 346(1−2): 292−301.

[22] XU X L, YU Z W, JI S J, SUN J C, HEI Z K. Differential scanning calorimetry and X-ray diffraction studies on aging behavior of Zn-Al alloys[J]. Acta Metallurgica Sinica (English letters), 2001, 14(2): 109−114.

[23] WANG K F, ZHAO X J. Characteristics of quench-aging process for ZA27 alloy[J]. Metals Heat Treatment Sinica, 1998, 5: 34−36.

[24] LI Z Q, WU B Y, ZHANG S Y. Solidification and microstructure of SiC/ZA-27composite fabricated by mechanical-electromagnetic combination stirring process[J]. Materials Science and Technology, 2001, 17(4): 465−471.

(Edited by LI Xiang-qun)